

## Thermal Transitions of Polyacrylonitrile Fibers

Paola Rizzo, Gaetano Guerra, and Finizia Auriemma\*

Dipartimento di Chimica, Università di Napoli Federico II, via Mezzocannone 4, I-80134 Naples, Italy

Received July 27, 1995

Revised Manuscript Received October 12, 1995

### Introduction

The thermal transitions of PAN have been characterized by several techniques. Dynamic-mechanical measurements show, in general, two main transitions close to 100 and 150 °C,<sup>1–4</sup> named by Minami  $\alpha_{II}$  and  $\alpha_I$  relaxations, respectively.<sup>4</sup>

The attribution of these transitions has not yet been entirely resolved.<sup>5</sup> According to some authors,<sup>1,6</sup> the two relaxations correspond to two glass transitions. In particular in ref 1, the presence of two phases, both essentially amorphous, is suggested and the phase contributing to the higher temperature relaxation is suggested to be of considerably higher order. These suggestions are mainly based on the activation energies obtained for the  $\alpha_{II}$  and  $\alpha_I$  relaxations, respectively.<sup>1</sup>

On the contrary, according to Minami and co-workers,<sup>2,4</sup> the high-temperature relaxation  $\alpha_I$  is due to the molecular motion in the amorphous region and the low-temperature absorption  $\alpha_{II}$  originates from the molecular motion in the paracrystalline region. This interpretation is mainly based on the dynamic-mechanical analysis on an amorphous PAN sample (obtained by using bis(pentamethylene imino)magnesium catalyst and having an isotactic predominant configuration<sup>2</sup>) which gives only one  $\tan \delta$  peak at 165 °C (at 110 Hz).

A thermal transition (hereafter referred to as a paracrystalline transition) has also been shown by X-ray diffraction measurements at different temperatures.<sup>3,7</sup> In particular, measurements at different temperatures of the X-ray  $d$  spacing of the main reflection of PAN (100) show that the thermal coefficient of lateral expansion of the pseudohexagonal unit cell changes around 85 °C. Dilatometric measurements also show the presence of a transition in the same temperature range.<sup>7,8</sup>

Although the paracrystalline transition (shown by the  $d$  spacing measurements) and the  $\alpha_{II}$  relaxation of the DMA scan occur at close temperature values, there is no evidence that the two transitions correspond to the same phenomenon.

In the present paper, DMA scans and X-ray diffraction measurements at different temperatures have been performed on as spun and annealed PAN fibers.

The aim is to elucidate the influence of the annealing on the  $\alpha_{II}$  transition, on the paracrystalline transition, and on the structure of PAN. The analysis is also aimed at contributing to the comprehension of the nature of the  $\alpha_{II}$  relaxation.

### Experimental Section

**Materials.** Two different PAN oriented samples are considered. Sample A is a commercial sample produced by Montefibre of Porto Marghera. It was produced by wet spinning from a 14% by weight dimethylacetamide solution. The fiber was stretched 14 times in a boiling water bath, the final diameter of each filament is close to 15  $\mu\text{m}$ .

Sample B is a laboratory sample prepared by the Montefibre Research Center of Porto Marghera. This sample was also obtained by wet spinning from a 14% by weight dimethyl-

acetamide solution, but the fiber was stretched only 2 times in a boiling water bath (the diameter of each filament is close to 40  $\mu\text{m}$ ).

Samples A and B present similar crystallinities but very different degrees of orientation. The half-widths of the equatorial main peaks along the azimuthal profile are 13 and 40°, for sample A and sample B, respectively.

The birefringence, determined using a Leitz polarizing microscope with an Ehringhaus rotary compensator of 5 orders, is 0.002 and 0.001 for samples A and B, respectively.

The annealing of sample A was carried out under vacuum at 140 °C for 2 h with free ends. Of course, the degree of orientation decreases with the thermal treatment: the half-width of the equatorial main peak along the azimuthal profile becomes 22°.

Before the measurements the as spun fibers have been humidity conditioned in a controlled temperature chamber with 65% relative humidity, maintained using a saturated  $\text{NH}_4\text{Cl}$  and  $\text{KNO}_3$  solution. The corresponding equilibrium moisture content, as determined by thermogravimetric analysis, is of nearly 2% by weight.

**Characterization Techniques.** The reported dynamic mechanical analysis (DMA) was carried out with a Polymer Laboratories DMTA apparatus at a measurement frequency of 10 Hz and at a heating rate of 1 °C/min. Bundles of fibers have been mounted in the bending mode as a double cantilever. The incomplete parallelism of the filaments and the inaccuracy in the determination of the sample section, which is subjected to the bending, reduce the accuracy of the measured moduli. However, a fair accuracy is reached for the measurement of the loss factor  $\tan \delta$  and, in particular, for the positions of the maxima (assumed as transition temperatures).

The measurements of the activation energies were performed by multifrequency scans at 0.3, 1, 3, 10, and 30 Hz, at a heating rate of 0.5 °C/min.

The X-ray diffraction patterns at different temperatures were obtained with an automatic Philips powder diffractometer (Ni-filtered  $\text{Cu K}\alpha$  radiation) with a temperature control of  $\pm 0.5$  deg.

For the X-ray diffraction measurements, in order to achieve a substantial disorientation of the samples, the fibers have been cut into short stretches (few millimeters) and spread in the holder. The diffraction intensity is measured by scanning the diffraction profile corresponding to the main diffraction peak (Miller indices (100),  $2\theta \approx 17^\circ$ ) with steps of 0.05° for 120 s/step; then the precise  $2\theta$  value corresponding to the maximum intensity is determined by interpolation. The method is particularly accurate in determining variations of the  $d$  spacing with the temperature, for a given sample. The absolute values of  $d$  can be indeed influenced by the coarseness of the shape and size of the sample and by effects of preferred orientation.<sup>9</sup>

The X-ray diffraction patterns at room temperature for the oriented fibers were obtained using a Nonius automatic X-ray diffractometer with Ni-filtered  $\text{Cu K}\alpha$  radiation and were collected, always maintaining an equatorial geometry. In this paper, only meridional scans (along  $\zeta$  for  $\xi = 0$ ) and numerical results relative to azimuthal scans for the main equatorial reflection are reported. The measurements were performed on bundles of fibers which were maintained parallel in a Lindemann capillary, and a subtraction of the diffraction halo of the capillary was necessary.

### Results and Discussion

The storage modulus,  $E'$ , and the loss factor,  $\tan \delta$ , of dry annealed sample A (highly drawn) and sample B (poorly drawn) are reported in Figure 1A,B, respectively. These DMA scans are analogous to those reported in the literature. In particular, a  $\tan \delta$  peak close to 150 °C is present for the poorly oriented sample (Figure 1B) but absent for the highly oriented one (Figure 1A).<sup>1,4</sup> For both samples, an increase of  $E'$  for  $T > 220$  °C corresponds to the cyclization reactions which occur in

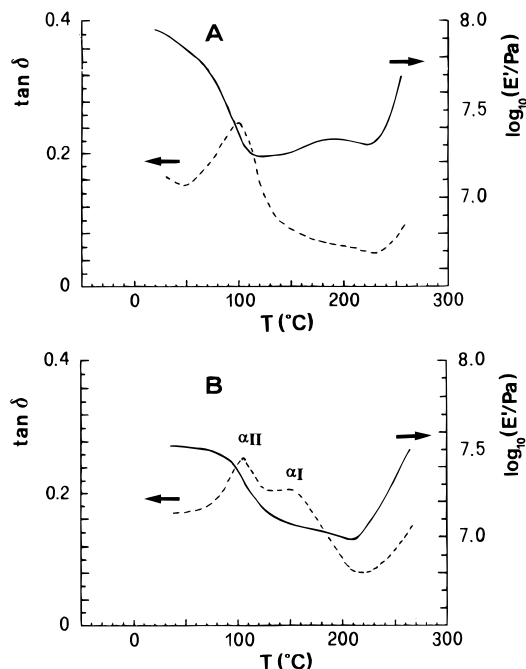


**Figure 1.** Storage modulus,  $E'$  (—), and loss factor,  $\tan \delta$  (---), from dynamic mechanical measurements, at a frequency of 10 Hz and at a heating rate of 1 °C/min, for dry annealed PAN fibers: (A) sample A (stretched 14 times); (B) sample B (stretched 2 times).

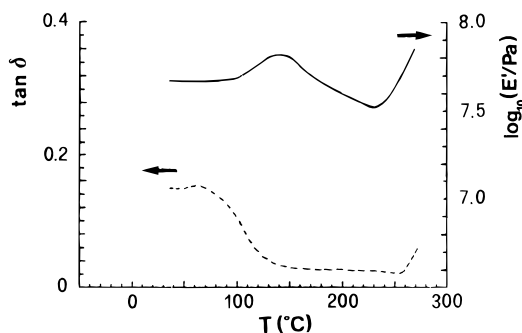


**Figure 2.** Storage modulus,  $E'$  (—), and loss factor,  $\tan \delta$  (---), from dynamic mechanical measurements, at a frequency of 10 Hz and at a heating rate of 1 °C/min starting from room temperature, for the wet unannealed PAN fiber sample A.

the thermostabilization processes leading to carbon fiber precursors.<sup>10,11</sup>

The storage modulus and the loss factor of the unannealed as spun sample A, after humidity conditioning, is reported in Figure 2.

By a comparison between Figures 1A and 2, it is apparent that the DMA scan of the highly drawn sample A is heavily changed by the annealing procedure. In particular, the main  $\tan \delta$  peak becomes more intense and is shifted from 63 °C to nearly 100 °C. It is also worth noting that, whereas for the dry annealed sample the  $\alpha_{II}$  relaxation is also pointed out by a drop of the modulus in the temperature range from room temperature to 110 °C, correspondingly, for the wet unannealed sample the modulus remains substantially constant up to nearly 100 °C and then slightly increases, reaching a maximum at nearly 140 °C. This increase of the modulus could be possibly due to the water desorption upon heating.

From DMA scans at five different frequencies different activation energies for the  $\alpha_{II}$  relaxation have been obtained for the annealed and unannealed fibers ( $3.5 \times 10^2$  and  $2.1 \times 10^2$  kJ/mol, respectively). The last

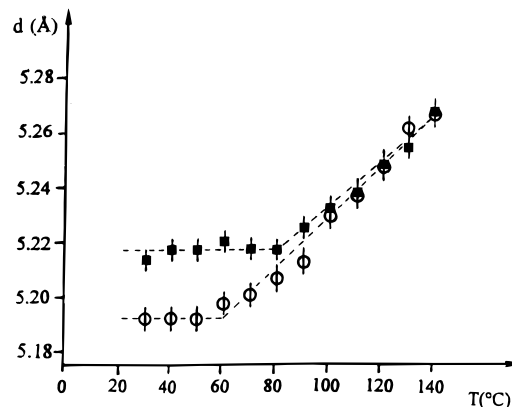


**Figure 3.** Temperature dependence of the lattice spacing ( $d$ ) calculated from the main reflection for the unannealed PAN fiber A: (○) heating; (■) cooling.

value is close to that one reported in the literature for the  $\alpha_{II}$  relaxation.<sup>1</sup>

It is worth noting that, contrary to a literature report,<sup>12</sup> the DMA scans of the annealed fibers of Figure 1 do not change after absorption of water. For instance, the  $\tan \delta$  peak temperatures of the fibers remain unchanged after immersion in water at 95 °C for 36 h (water content by thermogravimetry close to 3%).

The lattice spacings of the unannealed PAN fiber A, calculated from the position of the main reflection of the X-ray diffraction pattern, are plotted as a function of temperature in Figure 3. Circles and squares correspond to the X-ray diffraction data collected on heating to 140 °C and on cooling to room temperature, respectively. For repeated heating–cooling cycles (i.e., for annealed fibers) a behavior similar to that observed on cooling is obtained. For annealed fibers the observed behavior (cooling cycle) is analogous to that described in the literature:<sup>3,7</sup> above a transition temperature close to 80–85 °C, the coefficient of lateral expansion increases to  $2 \times 10^{-2}\%/deg$ .

For the unannealed PAN fiber A, the paracrystalline transition temperature, estimated by the intersection of the two lines interpolating the  $d$  data below and above the transition, is shifted down to nearly 60 °C.

It is also worth noting that at room temperature the interchain distance of the annealed fiber is larger by nearly 0.5% with respect to the unannealed fiber. Hence, the annealing of the as spun PAN fiber induces a structural change pointed out by the increase of the temperature of the paracrystalline transition as well as by the increase of the interchain distance.

A further aspect of the structural change due to the annealing is shown by a comparison of the meridional profiles (along  $\zeta$  for  $\xi = 0$ ) of the X-ray diffraction patterns of the annealed (Figure 4A) and unannealed (Figure 4B) fibers. Both profiles present a broad peak at  $\zeta \approx 0.29 \text{ \AA}^{-1}$ , which is only the tail of the halo centered at  $\xi \approx 0.15 \text{ \AA}^{-1}$  and  $\zeta \approx 0.25 \text{ \AA}^{-1}$ , typical of PAN;<sup>13–15</sup> the remaining peaks in Figure 4A,B are really meridional. Of course, the ratio between the intensity of the peak at  $\zeta \approx 0.29 \text{ \AA}^{-1}$  and the intensities of any other peak along the meridian increases with decreasing degree of orientation of the sample (compare Figure 4A,B). As for the peaks which are really meridional, the diffraction profiles of annealed and unannealed sample A both present a very broad meridional peak centered at  $\zeta \approx 0.79 \text{ \AA}^{-1}$ ; the annealed sample presents a broad peak centered at  $\zeta \approx 0.43 \text{ \AA}^{-1}$  corresponding to an average periodicity along the chain axis close to 2.3

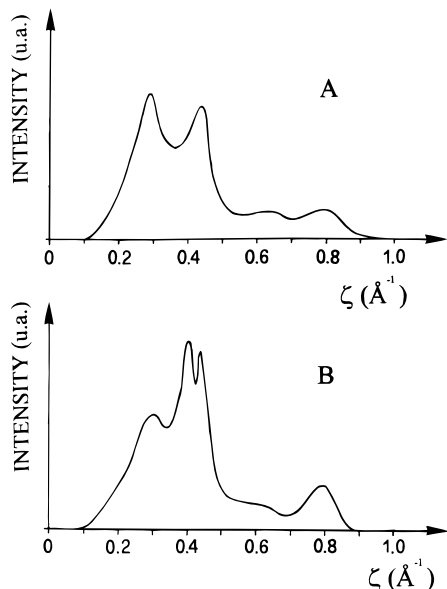


**Figure 4.** Meridional profiles (along  $\zeta$  for  $\xi = 0$ ) of the X-ray diffraction patterns of the annealed (A) and unannealed (B) fiber sample A.

Å; the unannealed fiber presents, instead, two narrower peaks centered at  $\zeta \approx 0.40 \text{ \AA}^{-1}$  and  $\zeta \approx 0.43 \text{ \AA}^{-1}$ , corresponding to periodicities close to 2.5 and 2.3 Å, respectively. Hence, the analysis of the meridional profiles indicates that the average unit height slightly decreases after the annealing procedure.

In summary, after the annealing procedure, an increase of the interchain distance associated with a reduction of the average periodicity along the chain axis is observed, which should leave substantially unaltered the density of the paracrystalline phase.

A comparison of the DMA and X-ray diffraction results for the considered PAN fiber is particularly informative. Upon annealing, the temperature corresponding to the  $\alpha_{II}$  relaxation of the DMA scan (at 10

Hz) is shifted from 63 to 100 °C and the paracrystalline transition temperature as obtained by the  $d$  vs  $T$  plots is roughly shifted from 60 to 80 °C. This suggests that the  $\alpha_{II}$  relaxation of the DMA scan and the paracrystalline transition shown by the  $d$  spacing measurements are related to the same phenomenon and confirms Minami's hypothesis that the  $\alpha_{II}$  relaxation of the DMA scan is relative to the paracrystalline phase.

**Acknowledgment.** The authors thank Dr. Raffaele Tedesco of the Montefibre SpA, di Porto Marghera, for useful discussions. This work was supported by the Ministero dell'Università e della Ricerca Scientifica e Tecnologica (Italy) and by the Consiglio Nazionale delle Ricerche. X-ray diffraction data were recorded with a Nonius CAD4 automatic diffractometer (Centro Interdipartimentale di Metodologie Chimico Fisiche, University of Naples).

#### References and Notes

- (1) Okajima, S.; Ikeda, M.; Takeuchi, A. *J. Polym. Sci., Polym. Chem. Ed.* **1968**, *6*, 1925.
- (2) Imai, Y.; Minami, S.; Yoshihara, T.; Joh, Y.; Sato, H. *J. Polym. Sci. Part B* **1970**, *8*, 288.
- (3) Hinrichsen, G. *J. Polym. Sci., Part C* **1972**, *38*, 303.
- (4) Minami, S. *Appl. Polym. Symp.* **1974**, *25*, 145.
- (5) Frushour, B. G.; Knorr, R. S. *Acrylic Fibers* **1984**, 171.
- (6) Andrews, R. D.; Kimmel, R. H. *J. Polym. Sci., Part B* **1965**, *3*, 167.
- (7) Bohn, C. R.; Schaeffgen, J. R.; Statton, W. O. *J. Polym. Sci.* **1961**, *55*, 531.
- (8) Krigbaum, W. R.; Tokita, N. *J. Polym. Sci.* **1960**, *43*, 467.
- (9) Klug, H. P.; Alexander, L. E. *X-ray Diffraction Procedures*; J. Wiley & Sons: New York, 1959.
- (10) Clarke, A. J.; Beiley, J. E. *Nature* **1971**, *234*, 529.
- (11) Clarke, A. J.; Beiley, J. E. *Nature* **1973**, *243*, 146.
- (12) Aitken, D.; Burkinshaw, S. M.; Cox, R.; Catherall, J.; Litchfield, R. E.; Price, D. M. *J. Appl. Polym. Sci., Appl. Polym. Symp.* **1991**, *47*, 263.
- (13) Hinrichsen, G.; Orth, H. *Kolloid-Z. Z. Polym.* **1971**, *247*, 844.
- (14) Liu, X. D.; Ruland, W. *Macromolecules* **1993**, *26*, 3030.
- (15) Rizzo, P.; Auriemma, F.; Guerra, G.; Petraccone, V.; Corradini, P. Submitted for publication to *Macromolecules*.

MA951099A